Extrusion-based technologies for 3D printing: a comparative study of the processability of thermoplastic polyurethane-based formulations.

Ángela Aguilar-de-Leyva, Vicente Linares*, Juan Domínguez-Robles, Marta Casas, Isidoro Caraballo

Department of Pharmacy and Pharmaceutical Technology, Faculty of Pharmacy, Universidad de Sevilla, C/Profesor García González 2, 41012 Seville, Spain.

*Corresponding author: vlinares@us.es

Extrusion-based technologies for 3D printing: a comparative study of the processability of thermoplastic polyurethane-based formulations.

Thermoplastic polyurethanes (TPU) offer excellent properties for a wide range of dosage forms. These polymers have been successfully utilized in personalized medicine production using Fused Deposition Modeling 3D printing (3DP). However, Direct Powder Extrusion (DPE) has been introduced recently as a challenging technique since it eliminates filament production before 3DP, reducing thermal stress, production time, and costs. This study compares DPE and single-screw extrusion for binary (drug-TPU) and ternary (drug-TPU-magnesium stearate) mixtures containing from 20 to 60 % w/w of theophylline. Powder flow, mechanical properties, fractal analysis and percolation theory were utilized to analyze critical properties of the extrudates. All the mixtures could be processed at a temperature range between 130 and 160ºC. Extrudates containing up to 50% w/w of drug (up to 30% w/w of drug in the case of single-screw extrusion binary filaments) showed toughness values above the critical threshold of 80 kg/mm^2. Magnesium stearate improved flow in mixtures where the drug is the only percolating component, reduced until 25 °C the DPE temperature and decreased the extrudate roughness in high drug content systems. The potential of DPE as an efficient one-step additive manufacturing technique in healthcare environments to produce TPU-based tailored on-demand medicines has been demonstrated.

Keywords: 3D printing; Thermoplastic Polyurethanes; Single Screw Extrusion; Direct Powder Extrusion; fractal analysis.

1. Introduction

3D printing technology is being widely applied in different industries such as automotive, construction, or aerospace. In the healthcare sector, it is applied to the production of dental apparatuses, implants, or even bone scaffolds. In the field of pharmacy, investigation related to 3D printing technologies is gaining an increasing interest due to the possibility that offers relationed with the production of personalised medicines (Aguilar-De-Leyva et al. 2020; Krueger et al. 2022)

3D printing is an additive manufacturing technology in which an object is constructed using computer-aided design software, sliced, and transferred to a printer where the product is constructed layer by layer using the principle of layered manufacturing (Wang et al. 2023). This way of producing medicines has the advantage of developing dosage forms with complex structures and geometries that are difficult to produce with conventional manufacturing methods. These products can be adjusted to the specific dose requirements, drug combinations or release profiles of different patiens based on their age, genetics or physiological conditions. This possibility is of special importance in the case of paediatric or geriatric patients (Parulski et al. 2021; Muhindo et al. 2023) .

Direct Powder Extrusion (DPE) is an additive manufacturing technique that relies on the feeding of a powder mixture into the printer, heating, extrusion and printing by deposition onto a building platform, layer by layer to create three-dimensional objects (Sánchez-Guirales et al. 2021) . One of the main advantages of this technique, compared to fused deposition modelling (FDM), is that it is not necessary to produce thermoplastic filaments (usually obteined by Hot Melt Extrusion (HME)) with suitable properties (nor too brittle neither too flexible) before the final step of 3D printing. This fact avoids complications when high drug doses are required, since HME needs a large amount of excipient to obtain adequate filaments. Furthermore, the impact of high temperatures, which can lead to drug degradation, is decreased, since the materials are subjected to a unique thermal process, allowing the use of drugs with lower degradation temperatures (Pistone et al. 2022). Therefore, this single-step manufacturing process helps to reduce time and cost in the production of drug delivery systems, making possible its implementation in hospital settings (Annaji et al. 2020; Malebari et al. 2022) .

Thermoplastic polyurethanes (TPU) have been widely employed in the production of different types of dosage forms such as vaginal rings or implants as well as in drug loaded cardiovascular prothesis, stents or medical tubing. Their inert, non-ionic and water-insoluble properties together with their high tensile strengh, highly elastomeric features and biocompatibility make these products very suitable for healthcare applications (Claeys et al. 2015). Recently, these polymers have been employed in the production of 3D printed drug loaded systems prepared by FDM (Verstraete et al. 2018; Domínguez-Robles et al. 2020; Arany et al. 2021; Domínguez-Robles et al. 2022). The study of the filaments for FDM has been carried out employing different tools such as percolation theory and fractal analysis (Linares et al. 2021; Linares et al. 2022).

Percolation theory, derived from the statistic physics, studies disordered or caotic systems in which the components are distributed in a network in a random way. The main concept of this theory is the percolation threshold, which is defined as the minimum concentration of a component at which there is a maximum probability of appearance of an infinite or percolating cluster of this material. A cluster is defined as a group of neighbour particles of the same component that share one side of the cell representing them on the grid. When a component starts to spread over the hole sample, it forms a percolating cluster. At this concentration point a geometrical phase transition takes place and this componet starts to exert a much stronger influence on the properties of the system. Abrupt changes in the properties of the systems are expected near this concentration point (Fuertes et al. 2006; Caraballo 2009; Caraballo 2010).

Euclidean geometry has been commonly used to describe mostly ordered systems and therefore does not fit well with more chaotic systems such as those found in nature (Pippa et al. 2013). It was the mathematician Benoit Mandelbrot who introduced the first mathematical model to describe geometrically the apparent irregularities of systems present in nature. Studying some natural objects at different magnifications, he realized that there is a symmetry, an invariant pattern independent of the scale used. Fractality is therefore defined by the presence of self-similarity, which is a property of an object or system to resemble itself at different scales (Young and Crawford 1991). This self-similarity gives the system different degrees of complexity and can be quantified thanks to the fractal dimension. Fractality analysis results in a value that determines the fractal dimension,

which relates the surface area or volume of an object and the scale at which it is being measured (Dillon et al. 2001).

Among the possible methods for studying the fractal dimension, one of the most popular is the box-counting method which has been previously employed by (Linares et al. 2021) according to the methodology proposed by (Dillon et al. 2001). This method assumes that the system to be analysed is covered by a square mesh of different sizes (λ), so that by counting the number of boxes (N) that contain part of the system, the value of the fractal dimension (D) can be obtained based on equation (1):

$$N(\lambda) = C\lambda^{-D} \qquad (1)$$

Where C is a proportionality constant.

The fractal dimension has been applied in pharmaceutical technology in several areas, such as the study of formulations with solid particles. Of particular relevance is the characterisation of the roughness of powders, and the impact this in turn has on the powder flow properties or bioavailability of pharmaceutical systems such as tablets (Thibert et al. 1988; Fernández-Hervás et al. 1994; Burnett et al. 2011; Abreu-Villela et al. 2019). More recently, it can be highlighted the application of the study of fractality in drug-loaded thermoplastic filaments which were used in FDM for the 3D printing of drug delivery systems. The roughness resulting from the analysis was related to the printability of the system (Linares et al. 2021; Mora-Castaño et al. 2022; Linares et al. 2022).

The aim of this work is to compare the processability of different types of binary and ternary TPU powder mixtures employing two different extrusion-based 3DP technologies: DPE and single-screw extrusion. Powder flow studies of the powder blends have been carried out and relationed with the extrusion process. Critical properties of the resulting extrudates have been studied using different approaches such as fractal analysis and percolation theory in order to compare both 3D printing technologies.

2. **Materials and Methods**

2.1. Materials

Anhydrous theophylline (AT), employed as model drug, was bought from Acofarma (batch 151209-P-1, Barcelona, Spain). Medical grade Tecoflex^{TM} EG-72D thermoplastic

polyurethane (TPU), used as a matrix forming polymer, was supplied by Lubrizol Advanced Materials (Barcelona, Spain). Magnesium stearate (MS) (mean diameter 20 μm), used as a lubricant, was purchased from Acofarma (batch 201081, Barcelona, Spain).

2.2. Methods

2.2.1. Preparation of the binary and ternary mixtures

TPU powder was obtained from previously frozen TPU pellets pulverized in a mill (Retsch ZM 200, Haan, Germany) using liquid nitrogen and a 1.0 mm output sieve. A 227.9 ± 166.0 μm mean diameter was obtained. AT with a mean diameter of 121.5 ± 45.0 μm was employed. The binary mixtures of AT and TPU powder and the ternary mixtures obtained after adding MS were blended for 15 min in a Turbula mixer (Willy A. Bachofen, Basel, Switzerland). The optimum mixing time was chosen according to a previously published work (Galdón et al. 2019). The composition of the different batches manufactured can be observed in Table 1.

2.2.2. Powder flow studies of binary and ternary powder blends

Different tests have been performed in order to characterize the powder flow of the mixtures prepared. Bulk density (q_{bulk}), tapped density (q_{tapped}), rest angle (α) and powder flow were measured in accordance with the methods described in the European Pharmacopoeia 11th Edition (section 2.9.34-36) (Council of Europe. European Directorate for the Quality of Medicines & Healthcare 2023) . Inter particle porosity (IP); Carr's Index (CI) and Hausner Ratio (HR) are derived from the following equations:

$$HR = q_{tapped} / q_{bulk} \quad (2)$$

$$IP = q_{tapped} - q_{bulk} / q_{tapped} \times q_{bulk} \quad (3)$$

$$CI = (q_{tapped} - q_{bulk} / q_{tapped}) \times 100 \quad (4)$$

2.2.3. Extrusion Process

All the physical mixtures were subjected to an extrusion process using both, a single screw Noztek Pro extruder (Noztek, Sussex, UK) and a DPE 3D printer M3dimaker (FabRx,

London, UK) at the temperatures recorded in Table 1. The conditions employed with the Noztek Pro extruder for all batches were a screw speed of 33 rpm, a diameter of the nozzle of 1.75 mm and a preheat of 30 min in order to establish thermal equilibrium before extrusion. With the aim of checking that the required diameter value of 1.75 mm for FDM 3D printing was obtained, the diameter of the filaments produced was measured using a digital micrometer (Comecta, SA, Barcelona, Spain).

In the case of the M3dimaker 3D printer, the parameters utilized were the maximum screw speed allowed, a nozzle diameter of 0.8 mm and a preheat of 15 min, as recommended by the fabricant. The diameter of the strands was also measured with a digital micrometer (Comecta, SA, Barcelona, Spain) in order to check the concordance with the nozzle diameter and the variability between different batches.

The extrudates produced for both methods were stored in an appropriate packaging at 25 ºC.

2.2.4. Thermal Analysis of the extrudates

Thermal properties of the pure materials and extrudates prepared by both techniques were evaluated using Differential Scanning Calorimetry (DSC) and Thermogravimetric Analysis (TGA) in order to study the stability and compatibility of the components utilized as well as their thermal decomposition.

DSC analyses were carried out in a DSC Q20 V24.11 Build 124 (TA Instruments, New Castle, DE, USA) in the Functional Characterization Service of the Center for Research, Technology, and Innovation of the University of Seville (CITIUS). Crimped hermetical aluminum pans were used to place about 2-12 mg of each sample that were heated from 30 ◦C to 300 ◦C at a heating rate of 5 ◦C/min under a dry nitrogen flow (100 mL/min).

TGA were performed in a thermal analyzer (SDT Q600 V20.9 Build 20, TA Instruments, New Castle, DE, USA) in the Functional Characterization Service of the University of Seville (CITIUS). About 4-11 mg of each sample were placed in an aluminum crucible and heated from room temperature to 600 ◦C employing a heating rate of 10 ◦C/min under a nitrogen gas purge of 100 mL/min.

DSC and TGA data were analyzed using Universal Analysis 2000 V4.5A software (TA Instruments, UK).

2.2.5. Scanning electron microscopy (SEM)

Scanning Electron Microscopy (SEM) was carried out in the Microscopy Service of the Center for Research, Technology, and Innovation of the University of Seville (CITIUS) to evaluate the surface of the extrudates obtained. A FESEM (Field Emission Scanning electron microscope) Schottky type (Thermofisher, Eindhoven, Holland) operating at 5 kV was used. A Leica ACE 600 high vacuum sputter coater was employed to coat the samples with a 10 nm-thin Pt layer before the analysis of the images.

2.2.6. Powder X-Ray diffraction (PXRD)

Powder X-ray diffractometry analysis (PXRD) were carried out to the pure components as well as to the binary and ternary strands containing 20 and 60% w/w of AT prepared by DPE. The X-ray diffraction patterns were collected with a Bruker D8 Advance A25 diffractometer (Karlsruhe, Germany) equipped with a lineal Lynexe detector with an opening of 3.3º. X-rays were generated with a copper anode operating at 40 kV and a current of 30 mA. The data were acquired over the 2θ range of 3º to 70º at a scanning step of 0.015º and measurement time of 0.1 s per step.

2.2.7. Mechanical properties of the extrudates

The stiffness of the filaments and strands was assessed using a Texture Analyser TA.XTPlus (Stable Micro Systems, Godalming, UK) at room temperature. Stiffness test following the previous methodology outlined by Xu *et al*., (Xu et al. 2020) was employed to measure the toughness of the performed extrudates. Briefly, five samples of each lot were cut into pieces of 6 cm in length and placed on the Texture Analyzer platform. Equipped with a set with knife blade, the Texture Analyzer was set to 50 g, and the blade was programmed to cut the extrudate piece until 1 mm in distance (57% strain) at a speed 2 mm/s. The maximum force and fracture distance were recorded by Texture Analyzer software, Texture Expert v.1.22 (Stable Micro Systems, Godalming, UK). Moreover, the Macro program in Texture Analyzer software was used to determine the area under curve (AUC) and maximum stress. Additionally, three anchors were inserted into the plot through the Macro program in the Texture Analyzer software. Anchor 1 marked the starting point of strain, anchor 2 represented the maximum strain, and anchor 3 indicated the end of the test when the stress

approached zero. The AUC between each pair of anchors was recorded. The sum of the AUC between anchor 1 & 2 and anchor 2 & 3 was defined as toughness and expressed in kg/mm^2.

2.2.8. Fractal analysis. Box-counting technique

The box-counting technique is based on the analysis of the perimeter of binary and ternary images, considering every pixel as a 'box'. Through this technique we can calculate the fractal dimension value. In this case, the roughness of the binary and ternary extrudates was studied by taking photographs with a stereo microscope SMZ800N (Nikon Instruments Inc., New York, USA). Images of each extrudate containing different drug content were taken with different zoom ratios (1x to 8x). Pixel modification was carried out thanks to the Nikon software (Nis-Elements BR 5.20.02) by increasing the pixel size ten times more than the original one (800x and 80x). This software was also used to binarize each photography. The measured perimeter in pixels was obtained with Matlab R2019b (The MathWorks, Inc., Massachusetts, USA). Pixels were converted into centimeters (cm) thanks to the Nikon software conversion pixel/cm. Thirty-six images were studied for each extrudate obtained entailing a total of 360 images analyzed.

2.3. Statistical analysis

All data were expressed as mean ± standard deviation. Data were compared using an unpaired *t*-test. In all cases, $p < 0.05$ was the minimum value considered acceptable for rejection of the null hypothesis.

3. Results and discussion

Powder flow of the binary and ternary powder blends were characterized and the results are shown in Table 2.

As it can be deduced from the results of binary mixtures assayed, the flow properties (HR and rest angle) worsen as the percentage of AT increases. Even, regarding the powder flow test, blends were unable to flow through the funnel, confirming their poor flow properties. The powder flow behaviour of AT particles has been previously evaluated by our group, making patent the low flowability of the drug, due to their fine size, acicular shape and electrostatic charge (Galdón et al. 2016). Moreover, the discontinuities of behaviour observed in the powder flow parameters with respect to AT ratio can be explained

according to the percolation theory. As this theory has demonstrated, powder blends behave as non-continuous systems. This way, these systems can suffer changes in their properties near to geometrical phase transitions of the components (Galdón et al. 2016). In that study, percolation thresholds have been estimated for AT powder blends. So, below 35.3% v/v concentration, the blends show better flow capacity, due to the predominant effect of the excipient. On the other hand, above 71.3% v/v, when mixtures contain only finite clusters of the excipient, the flowability parameters worsen due to the higher influence of AT. An estabilization of the flow parameters is observed for intermediate concentrations, when a bicoherent system with percolating clusters of drug and excipient is obtained. Figure 1 shows the HR, IP and CI values for powder mixtures where the influence of AT concentration on flow properties becames clear in binary blends. The trend observed in this parameter, where the values increase, stabilize and then increase again, could agree with the percolation thresholds commented before. On the contrary, in the case of ternary mixtures, results do not show a change in their behaviour as a function of the concentration of AT, but more similar values, due to the presence of MS that masks the negative effect of AT in the blends where the drug is the only percolating component, improving the flow properties of the mixture. Surprisingly, MS seem to mask also the positive effects of TPU in the blends where TPU is the predominating component. A possible explanation could be the higher surface area that can favor the interparticulate interactions between MS and TPU. This could result in higher cohesion between the particles and therefore in poor flow. These phenomena are not signifficant when AT is predominant, possibly because AT crystalline particles are unlikely to bond by Van der Waals forces. Another reason could be that the higher density of AT particles resulted in a prevalence of gravitational forces over Van der Waals forces.

With respect to the extrusion process, all the powder mixtures could be extruded satisfactorily with the two methods tested. The extrusion process in the Noztek Pro extruder was carried out at 130 ºC for binary mixtures. In the case of ternary mixtures, the extrusion temperature decreased from 150 ºC to 135 ºC as the AT concentration increased. This fact could be attributed to the plasticizing effect of AT that has been previously reported (Okwuosa et al. 2016) in combination with the lubricant effect of MS.

The selection of the temperature was conditioned to the need of obtaining a filament diameter of 1.75 ± 0.1 mm, appropriated to allow the drive wheels of the FDM printer to print accurately (Linares et al. 2021). A suitable diameter was obtained for the binary filaments (1.69–1.82 mm) as well as for the ternary filaments (1.70–1.78 mm). Batches Bin30 and Bin40 constituted an exception since they had a sightly thinner diameter than the lower limit (1.56–1.64 mm).

In the case of DPE, the diameter of the strand obtained does not condition the printing process since it does not have to pass through the drive wheels but is printed directly. Therefore, the selection of the temperature is not conditioned by this factor. Nevertheless, the systems extruded showed very low variations in the diameter, being all the strands extruded in the range of 0.80-0.90 mm (mean diamente value of 0.84± 0.04 mm in the case of binary samples and 0.83 ± 0.04 mm for ternary samples). These data show a very good concordance with the nozzle diameter.

Binary and ternary batches containing 20-40% of AT were extruded at the same temperature. However, for mixtures containing 50 and 60% of AT, it was observed that the addition of MS allowed to reduce the extrusion temperature from 150ºC and 160ºC, respectively, to 135ºC. Therefore, the tendence in ternary mixtures is a decrease in the extrusion temperature when the percentage of AT increases, in the same way that occurs with the Noztek extruder. This way, it has been demonstrated that the use of a lubricant facilitates the DPE process allowing to employ lower temperatures. This fact is of great importance since it permits to work with a wider range of drugs in comparison to FDM .

SEM images were employed to analyze the morphology of the surface of the extrudates obtained (see Figure 2).

As it can be appreciated, in the case of Bin20 extrudates, a much rougher surface has been obtained for the strands obtained by DPE. This fact can be attributed to the lower time that the mixture is subjected to the high temperature (due to the lower length of the screw in the case of the DPE) and to the lower torque that the DPE has, in comparison with the Noztek extruder. Regarding ternary extrudates, Ter20 and Ter60 DPE strands show a clearly softer surface when compared with the same binary strands produced by DPE, due to the presence

of MS. This effect has been previously appreciated in the case of filaments produced by the Noztek (Linares et al. 2022).

Powder X-ray diffraction analysis were carried out for the strands prepared by DPE (Figure 3). A partial amorphization of the AT inside the strands has been produced since the diffractograms show an important decrease in the intensity of the larger peak of the drug at 12.8º, even when corrected with the proportion of the drug in the formulations. As a consequence of this phenomenon an increase in the solubilzation of the drug is expected, which could be benefitial in the case of BCS II and IV drugs.

In order to further investigate the results obtained from the PXRD diffractograms and evaluate the possible interactions between the TPU, MS (in the case of ternary mixtures) and AT in the different extrudates, thermal analysis were conducted. In the DSC thermogram it can be observed that the pure AT shows an endothermic peak at around 273ºC (see Figure 4) which corresponds to its melting point, characteristic of its crystalline state. This sharp melting endotherm is not observed for the different extrudates analyzed, suggesting that the crystalline form of the pure drug is converted to the amorphous form and a solid dispersion is obtained during both extrusion process. Similar results were previously found for filaments prepared with the same components (Linares et al. 2021).

TGA analysis were performed with the aim of studying the degradation profile of the pure components and the extrudates. As it can be observed in Figure 5, extrudates with the higher drug load show higher degradation with a weight loss of about 50% w/w at 300 ºC versus about 70-80% w/w of weight loss exhibited by extrudates with the lower drug content. Nevertheless, the weight loss for all the extrudates studied start above 250 ºC thus proving that all the extrudates are processed below their degradation temperatures.

In relation with the mechanical properties, a stiffness test was performed to evaluate the mechanical properties of both binary and ternary extrudates. This test is used to determine the toughness of the filaments, which is also linked to their printability by using FDM 3D printing technology. It has been stated that toughness values below 80 kg/mm^2 may lead to 3D printing difficulties by FDM (Xu et al. 2020). Figure 6 shows that toughness values of both binary and ternary strands containing the same percentage of AT prepared by DPE were quite close between them. Unlike what has been reported in previous studies (Linares

et al. 2022), the inclusion of MS in ternary strands did not provide any significative difference in their toughness values ($p > 0.05$). However, it had a significant impact on the extrusion temperature. For ternary formulations, including the MS, the extrusion temperature decreased as the AT concentration increased.

Toughness values of the strands were reduced when the AT% of the formulations was increased, especially when AT is percolating the system, i.e. above 40 % w/w AT, which correlates with more than 35% v/v (Aguilar-de-Leyva et al. 2015), regardless of the mixture type (binary or ternary mixtures) (Figure 6). However, all the performed formulations excluding 60% w/w of AT for both type of strands exhibited toughness values above the critical threshold (80 kg/mm^2).

In the case of the filaments prepared with the Noztek extruder, the values of binary and ternary filaments containing the same percentage of AT showed significative differences for 40 and 50% of AT ($p < 0.05$). Ternary filaments showed a behavior similar to the ternary DPE filaments with toughness values above 80 kg/mm^2 for filaments containing up to 50 % AT. However, binary filaments containing more than 30% exhibited toughness values below 80 kg/mm^2. Therefore, it can be stated that DPE produced strands with better toughness despite the fact of having finer diameters.

Morphological analysis of the strands obtained by DPE was carried out based on the fractal analysis. The box-counting technique was applied to analyse the strands' roughness from perimeter images (Dillon et al. 2001). Firstly, 36 images from 3 different parts of the binary and ternary strand for each batch (20–60% of drug content) were taken by the stereo microscope, giving a total of 360 images. These images were subjected to a binarization process to reduce the information available in the photograph and thus facilitate the analysis of the areas of interest. During this process, the image is transformed into binary data, where true and false are represented as values of 1 and 0, respectively, and represented as black and white images (Figure 7). The analysis of the images was performed with Matlab, which is able to detect the perimeter of the strand and determine the number of pixels that make up the strand. The perimeter photograph only captures one side of the strand, which simplifies the detection and analysis process for Matlab. After converting the perimeter measurement into centimetres, this value was plotted against the

inverse of the zoom ratio (1/1 to 1/8) (Figure 8). As a result, the fractal dimension value was obtained from the corresponding exponent of each equation (Table 3).

Taking into account that we are analysing in 2 dimensions the roughness of the strands, the maximum possible theoretical value is 2. In addition, the closer the value of the fractal dimension is to 1, the smoother the system is, or in other words, the less rough. In our case most values will be around 1. The results shown in Table 3 were plotted against the percentage of AT for binary and ternary strands (Figure 9a). As a result, we can observe in the graphical representation a general trend for both types of strands; as the amount of AT increases, the roughness increases as expected. Regarding the ternary strands, the roughness values in the 50 % and 60 % drug mixtures have a lower value than in the binary ones due to the presence of MS. Furthermore, another evident effect that MS has on ternary strands is the smoothing of roughness, so that the strands tend to have similar fractal dimension values as can be shown in the graph.

With respect to binary strands, as mentioned above, the more drug the strand contains, the higher the roughness. Here, the effect is further enhanced because the MS does not smooth the surface. Also, the jump that occurs in both types of strands from 50% of drug is remarkable. This indicates that it is a critical value from which roughness is magnified, the presence of AT becomes much more evident, and it has consequences on the mechanical properties of both strands, as indicated by the results of the stiffness test analysis.
The results of the fractal analysis of the strands are consistent with the results obtained from filaments produced using the same materials through single-screw extrusion (Figure 9b). Binary filaments manufactured through extrusion exhibited the same upward trend as the amount of drug increases, as observed in the case of binary strands made with DPE. Regarding ternary filaments made by extrusion, they show a tendency to have more homogeneous values. Although they are not the same machines, both extrusion and DPE involve a common process in which a powder mass is heated and pushed through a heated nozzle, resulting in extrudates with similar roughness properties and similar implications for mechanical properties. This is evident as there is also a change in stiffness values

associated with the higher amount of AT present in the extrudates. This ultimately has implications for the 3D printing process.

4. Conclusions

Both binary and ternary mixtures based in TPU have proved to be suitable to be processed by DPE and single screw extrusion, including those having a high drug concentration.

The presence of MS masks the negative effect of AT in the blends where the drug is the only percolating component, improving the flow properties and reducing the extrusion temperature until 25ºC in the case of DPE.

Regarding the roughness of the extrudates obtained, we can confirm that the presence of lubricant softens the surface of the systems with a higher content of AT, showing all the ternary batches obtained by both techniques similar fractal dimension values.

Binary strands obtained by DPE showed better toughness values, in spite of the lower torque that applies this technology in comparison with the single screw extruder.

DPE has demonstrated to be an adequate technology to process TPU formulations, which have been lately employed in the production of different dosage forms due to their favourable features. This technology showed important advantages such as the reduced impact of high temperatures as well as its simplification to a one-step process. Therefore, DPE is a valuable option to be implemented in healthcare settings for the production of customized on-demand drug delivery systems.

Acknowledgements

We thank Ministerio de Ciencia, Innovación y Universidades of Spain (Grant RTI2018 095041-B-C31) for financial support. This work has been supported by a PIF VI PPIT-US grant of the Universidad de Sevilla. This work has been financially supported from the Ramón y Cajal grant RYC-2021-034357-I funded by MCIN/AEI/10.13039/501100011033 and by the “European Union NextGenerationEU/PRTR”.

Declaration of interest statement

The authors declare that they have no known competing financial interests or personal relationships that could have appeared to influence the work reported in this paper.

References

Abreu-Villela RK& IC, Kuentz M, Caraballo I. 2019. Benefits of Fractal Approaches in Solid Dosage Form Development. Pharm Res. 36(156).

Aguilar-de-Leyva A, Campiñez MD, Casas M, Caraballo I. 2015. Critical Points and Phase Transitions in Polymeric Matrices for Controlled Drug Release. In: Kumar Thakur V, Kumari Thakur M, editors. Handbook of Polymers for Pharmaceutical Technologies. Vol. 1. Volume 1. Beverly MA: Scrivener Publishing. https://doi.org/10.1002/9781119041375.ch4

Aguilar-De-Leyva Á, Linares V, Casas M, Caraballo I. 2020. 3D Printed Drug Delivery Systems Based on Natural Products. Pharmaceutics [Internet]. 12:620. https://doi.org/10.3390/pharmaceutics12070620

Annaji M, Sindhu R, Poudel I, Govindarajulu M, Arnold RD, Dhanasekaran M, Babu RJB. 2020. Application of Extrusion-Based 3D Printed Dosage Forms in the Treatment of Chronic Diseases. J Pharm Sci. 109(12):3551–3568.

Arany P, Papp I, Zichar M, Regdon G, Béres M, Szalóki M, Kovács R, Fehér P, Ujhelyi Z, Vecsernyés M, Bácskay I. 2021. Manufacturing and Examination of Vaginal Drug Delivery System by FDM 3D Printing. Pharmaceutics [Internet]. [accessed 2023 Jun 10] 13(10):1714. https://doi.org/10.3390/pharmaceutics13101714

Burnett DJ, Heng JYY, Thielmann F, Garcia AR, Naderi M, Acharya M. 2011. Measuring Surface Roughness of Pharmaceutical Powders Using Vapor Sorption Methods. AAPS PharmSciTech. 12(1):56–61. https://doi.org/10.1208/s12249-010-9571-0

Caraballo I. 2009. Critical points in the formulation of pharmaceutical swellable controlled release dosage forms-Influence of particle size. Particuology. 7:421–425. https://doi.org/10.1016/j.partic.2009.10.002

Caraballo I. 2010. Factors affecting drug release from hydroxypropyl methyl cellulose matrix systems in the light of classical and percolation theories. Expert Opin Drug Deliv. 7(11):1291–1301.

Claeys B, Vervaeck A, Hillewaere XKD, Possemiers S, Hansen L, De Beer T, Remon JP, Vervaet C. 2015. Thermoplastic polyurethanes for the manufacturing of highly dosed oral sustained release matrices via hot melt extrusion and injection molding. European Journal of Pharmaceutics and Biopharmaceutics. 90:44–52. https://doi.org/10.1016/J.EJPB.2014.11.003

Council of Europe. European Directorate for the Quality of Medicines & Healthcare. 2023. European Pharmacopoeia. 11th edition.

Dillon CG, Carey PF, Worden RH. 2001. Fractscript: A macro for calculating the fractal dimension of object perimeters in images of multiple objects. Comput Geosci. 27(7):787–794. https://doi.org/10.1016/S0098-3004(00)00171-0

Domínguez-Robles J, Mancinelli C, Mancuso E, García-Romero I, Gilmore BF, Casettari L, Larrañeta E, Lamprou DA. 2020. 3D Printing of Drug-Loaded Thermoplastic Polyurethane Meshes: A Potential Material for Soft Tissue Reinforcement in Vaginal Surgery. Pharmaceutics [Internet]. [accessed 2023 May 30] 12(1):63. https://doi.org/10.3390/pharmaceutics12010063

Domínguez-Robles J, Utomo E, Cornelius VA, Anjani QK, Korelidou A, Gonzalez Z, Donnelly RF, Margariti A, Delgado-Aguilar M, Tarrés Q, Larrañeta E. 2022. TPU-based antiplatelet cardiovascular

prostheses prepared using fused deposition modelling. Mater Des. 220:110837. https://doi.org/10.1016/J.MATDES.2022.110837

Fernández-Hervás MJ, Holgado MA, Rabasco AM, Fini A. 1994. Use of fractal geometry on the characterization of particles morphology: Application to the diclofenac hydroxyethylpirrolidine salt. Int J Pharm. 108(3):187–194. https://doi.org/10.1016/0378-5173(94)90127-9

Fuertes I, Miranda A, Millán M, Caraballo I. 2006. Estimation of the percolation thresholds in acyclovir hydrophilic matrix tablets. European journal of pharmaceutics and biopharmaceutics. 64(3):336–42. https://doi.org/10.1016/j.ejpb.2006.05.009

Galdón E, Casas M, Caraballo I. 2019. Achieving High Excipient Efficiency with Elastic Thermoplastic Polyurethane by Ultrasound Assisted Direct Compression. Pharmaceutics [Internet]. 11(157). https://doi.org/10.3390/pharmaceutics11040157

Galdón E, Casas M, Gayango M, Caraballo I. 2016. First study of the evolution of the SeDeM expert system parameters based on percolation theory: Monitoring of their critical behavior. European Journal of Pharmaceutics and Biopharmaceutics. 109:158–164. https://doi.org/10.1016/j.ejpb.2016.10.004

Krueger L, Miles JA, Popat A. 2022. 3D printing hybrid materials using fused deposition modelling for solid oral dosage forms. Journal of Controlled Release. 351:444–455. https://doi.org/10.1016/J.JCONREL.2022.09.032

Linares V, Aguilar-de-Leyva Á, Casas M, Caraballo I. 2022. 3D Printed Fractal-like Structures with High Percentage of Drug for Zero-Order Colonic Release. Pharmaceutics [Internet]. [accessed 2023 May 30] 14(11):2298. https://doi.org/10.3390/pharmaceutics14112298

Linares V, Galdón E, Casas M, Caraballo I. 2021. Critical points for predicting 3D printable filaments behaviour. J Drug Deliv Sci Technol. 66:102933. https://doi.org/10.1016/J.JDDST.2021.102933

Malebari AM, Kara A, Khayyat AN, Mohammad KA, Serrano DR. 2022. Development of Advanced 3D-Printed Solid Dosage Pediatric Formulations for HIV Treatment. Pharmaceuticals. 15(4). https://doi.org/10.3390/ph15040435

Mora-Castaño G, Millán-Jiménez M, Linares V, Caraballo I. 2022. Assessment of the Extrusion Process and Printability of Suspension-Type Drug-Loaded Affinisol TM Filaments for 3D Printing. Pharmaceutics [Internet]. 14(4):1–17. https://doi.org/10.3390/pharmaceutics14040871

Muhindo D, Elkanayati R, Srinivasan P, Repka MA, Ashour EA. 2023. Recent Advances in the Applications of Additive Manufacturing (3D Printing) in Drug Delivery: A Comprehensive Review. AAPS PharmSciTech. 24(2). https://doi.org/10.1208/s12249-023-02524-9

Okwuosa TC, Stefaniak D, Arafat B, Isreb A, Wan KW, Alhnan MA. 2016. A Lower Temperature FDM 3D Printing for the Manufacture of Patient-Specific Immediate Release Tablets. Pharm Res. 33(11):2704–2712. https://doi.org/10.1007/s11095-016-1995-0

Parulski C, Jennotte O, Lechanteur A, Evrard B. 2021. Challenges of fused deposition modeling 3D printing in pharmaceutical applications: Where are we now? Adv Drug Deliv Rev. 175:113810. https://doi.org/10.1016/J.ADDR.2021.05.020

Pippa N, Dokoumetzidis A, Demetzos C, Macheras P. 2013. On the ubiquitous presence of fractals and fractal concepts in pharmaceutical sciences: A review. Int J Pharm. 456(2):340–352. https://doi.org/10.1016/J.IJPHARM.2013.08.087

Pistone M, Racaniello GF, Arduino I, Laquintana V, Lopalco A, Cutrignelli A, Rizzi R, Franco M, Lopedota A, Denora N. 2022. Direct cyclodextrin-based powder extrusion 3D printing for one-step production of the BCS class II model drug niclosamide. Drug Deliv Transl Res. 12(8):1895–1910. https://doi.org/10.1007/s13346-022-01124-7

Sánchez-Guirales SA, Jurado N, Kara A, Lalatsa A, Serrano DR. 2021. Understanding direct powder extrusion for fabrication of 3d printed personalised medicines: A case study for nifedipine minitablets. Pharmaceutics. 13(10). https://doi.org/10.3390/pharmaceutics13101583

Thibert, Akbarieh M, Tawashi R. 1988. Application of fractal dimension to the study of the surface ruggedness of granular solids and excipients. J Pharm Sci. 77(8):724726.

Verstraete G, Samaro A, Grymonpré W, Vanhoorne V, Van Snick B, Boone MN, Hellemans T, Van Hoorebeke L, Remon JP, Vervaet C. 2018. 3D printing of high drug loaded dosage forms using thermoplastic polyurethanes. Int J Pharm. 536(1):318–325. https://doi.org/10.1016/J.IJPHARM.2017.12.002

Wang S, Chen X, Han X, Hong X, Li X, Zhang H, Li M, Wang Z, Zheng A. 2023. A Review of 3D Printing Technology in Pharmaceutics: Technology and Applications, Now and Future. Pharmaceutics [Internet]. [accessed 2023 May 29] 15(2):416. https://doi.org/10.3390/pharmaceutics15020416

Xu P, Li J, Meda A, Osei-Yeboah F, Peterson ML, Repka M, Zhan X. 2020. Development of a quantitative method to evaluate the printability of filaments for fused deposition modeling 3D printing. Int J Pharm. 588:119760. https://doi.org/10.1016/J.IJPHARM.2020.119760

Young IM, Crawford JW. 1991. The fractal structure of soil aggregates: its measurement and interpretation. Journal of Soil Science. 42(2):187–192. https://doi.org/10.1111/j.1365-2389.1991.tb00400.x

Table 1. Composition and extrusion temperature of the studied batches.

	Bin20	**Bin30**	**Bin40**	**Bin50**	**Bin60**	**Ter20**	**Ter30**	**Ter40**	**Ter50**	**Ter60**
AT (% w/w)	20	30	40	50	60	20	30	40	50	60
TPU (% w/w)	80	70	60	50	40	75	65	55	45	35
MS (% w/w)	0	0	0	0	0	5	5	5	5	5
Noztek extrusion temperature (° C)	130	130	130	130	130	150	145	135	135	135
DPE extrusion temperature (° C)	150	145	135	150	160	150	145	135	135	135

AT: Theophylline anhydrous

TPU: Thermoplastic Polyurethane

MS: Magnesium stearate

Bin20-Bin60: binary extrudates containing from 20 to 60 % w/w of AT

Ter20-Ter60: ternary extrudates containing from 20 to 60 % w/w of AT

Table 2. Powder flow results from binary and ternary mixtures.

Batch	q_{bulk} (g/ml)	q_{tapped} (g/ml)	IP	CI (%)	HR	α (°)
Bin20	0.300±0.002	0.360±0.003	0.558±0.020	16.72±0.55	1.201±0.008	45.2±0.5
Bin30	0.304±0.002	0.379±0.003	0.646±0.020	19.66±0.12	1.245±0.002	54.9±1.6
Bin40	0.307±0.002	0.398±0.003	0.745±0.000	22.83±0.92	1.296±0.015	53.8±1.1
Bin50	0.310±0.002	0.407±0.003	0.767±0.034	23.77±1.06	1.312±0.018	53.1±1.0
Bin60	0.317±0.002	0.455±0.004	0.956±0.039	30.33±0.19	1.435±0.004	55.3±1.2
Ter20	0.335±0.002	0.429±0.006	0.656±0.038	21.93±1.22	1.281±0.020	51.0±2.3
Ter30	0.345±0.004	0.445±0.004	0.652±0.051	22.47±1.52	1.290±0.025	53.8±1.1
Ter40	0.358±0.002	0.463±0.004	0.635±0.000	22.71±0.16	1.294±0.003	49.5±0.9
Ter50	0.390±0.003	0.497±0.005	0.554±0.020	21.58±0.69	1.275±0.011	49.6±0.7
Ter60	0.401±0.003	0.528±0.000	0.597±0.020	23.96±0.60	1.315±0.010	46.0±0.8

Table 3. Fractal dimension values defined by the equation of the graph from different drug contents.

% AT	Regression Equation	Binary Fractal Dimensión	Regression Equation	Ternary Fractal Dimension
20	$y = 0.4176^{-1.006}$	1.006	y = 0.4235-1.022	1.022
30	$y = 0.4308^{-1.011}$	1.011	y = 0.4226-1.015	1.015
40	$y = 0.4247^{-1.013}$	1.013	y = 0.4073-1.018	1.018
50	$y = 0.4624^{-1.057}$	1.057	y = 0.3900-1.03	1.03
60	$y = 0.4014^{-1.054}$	1.054	y = 0.4274-1.025	1.025

Figures

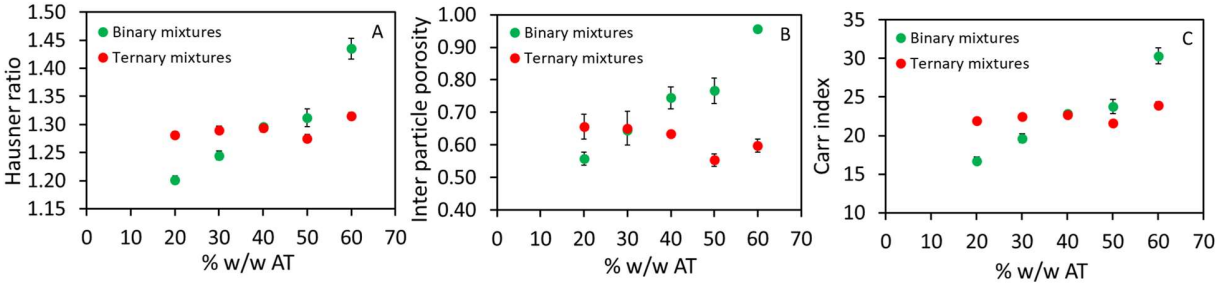

Figure 1.

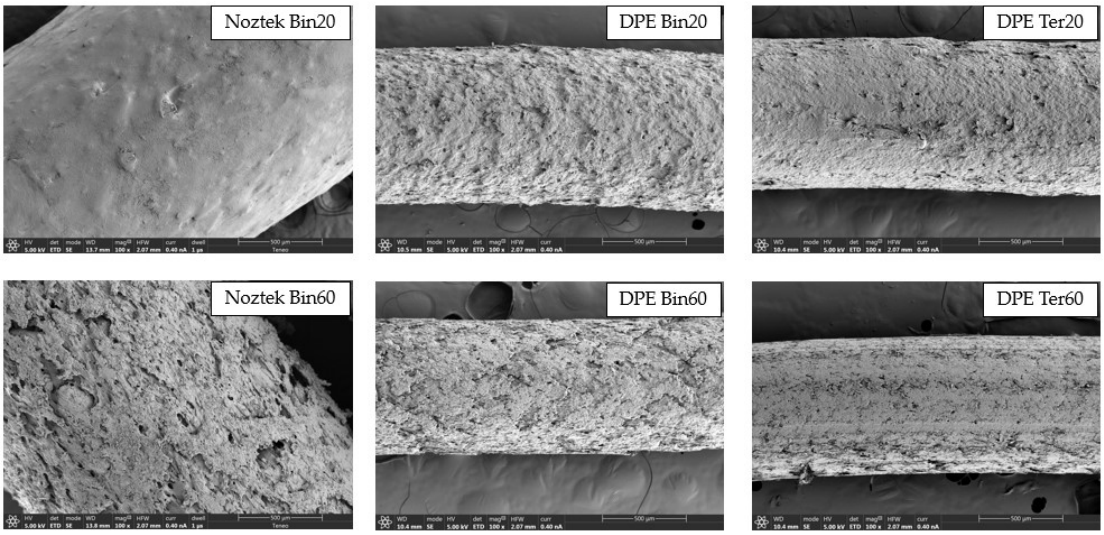

Figure 2.

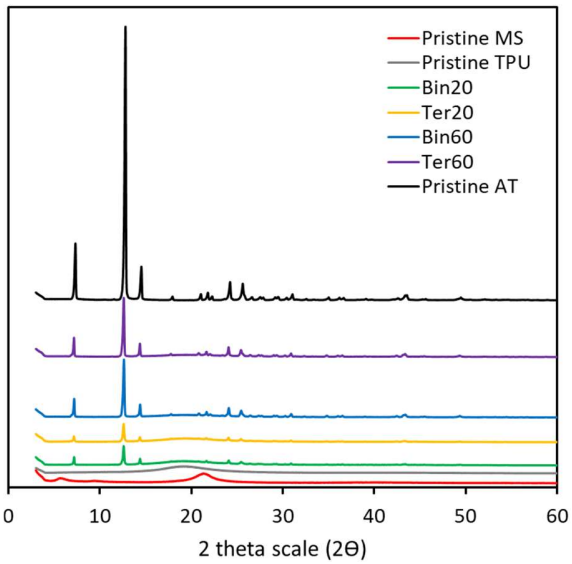

Figure 3.

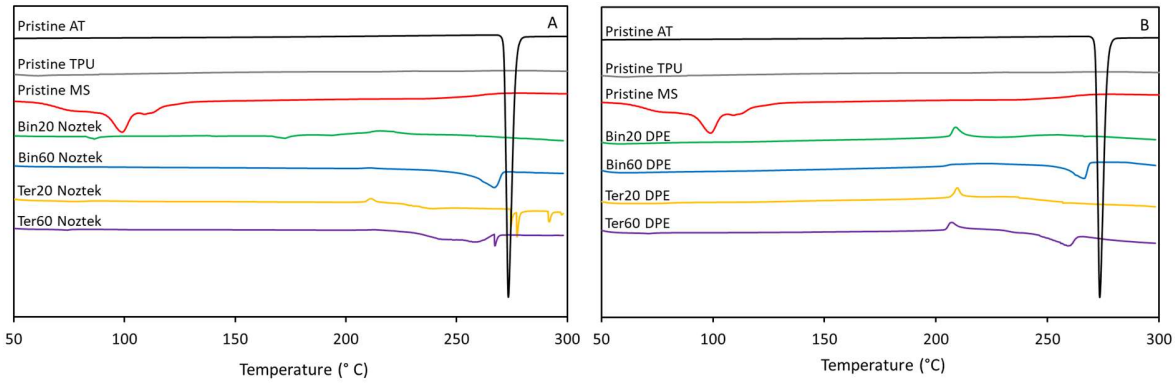

Figure 4.

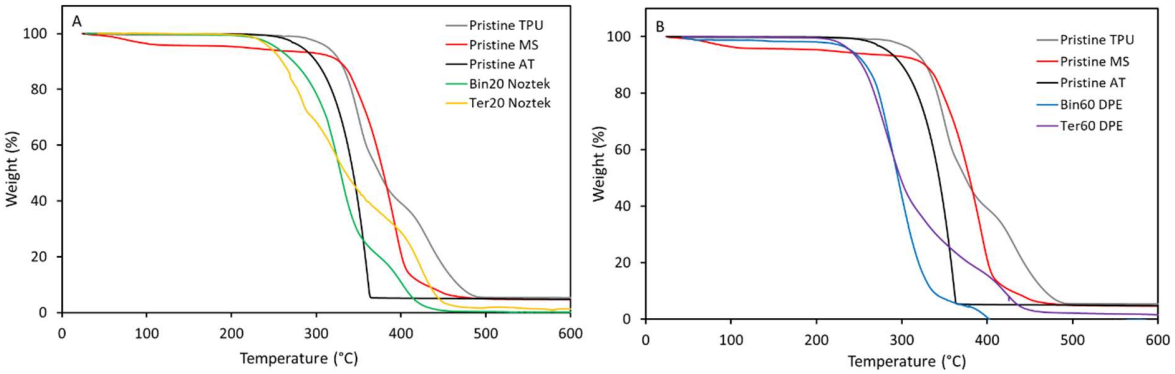

Figure 5.

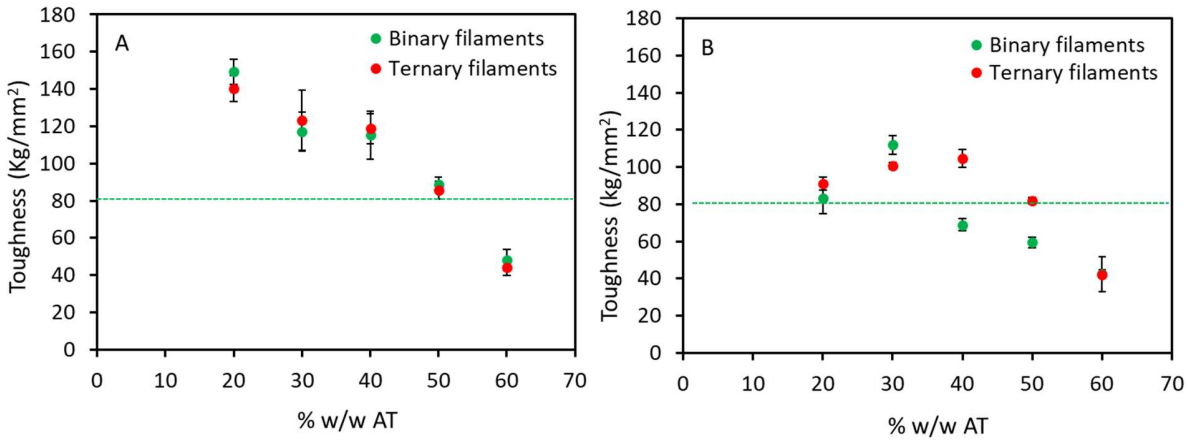

Figure 6.

Figure 7.

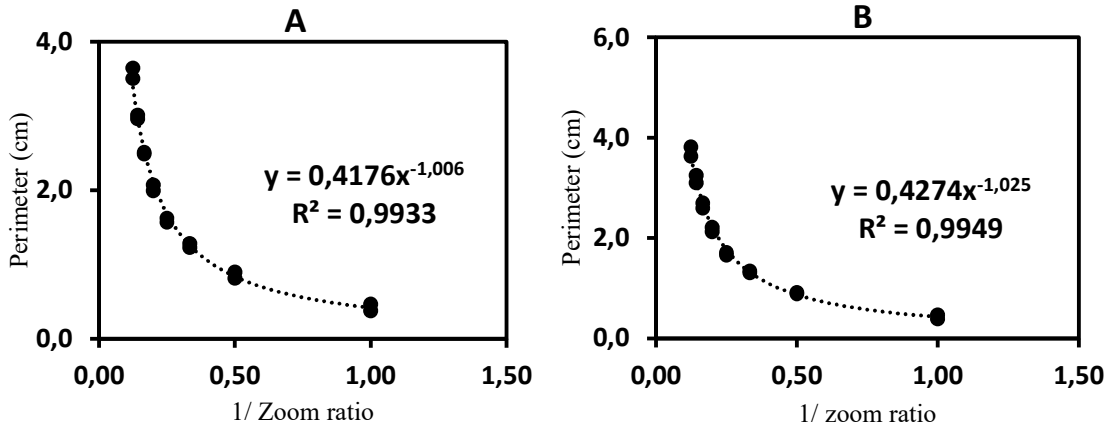

Figure 8.

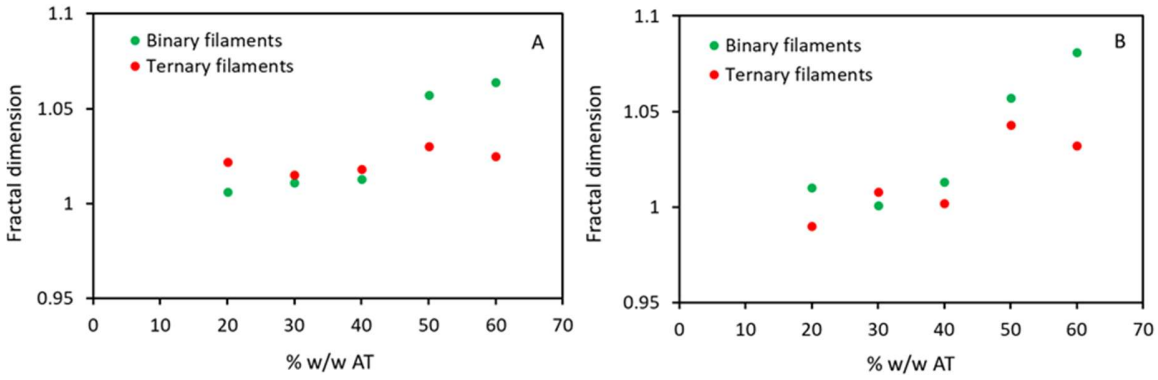

Figure 9.

Figure captions

- Figure 1. Powder flow parameters for the powdered binary and ternary mixtures: Hausner ratio (A); Inter particle porosity (B) and Carr Index (C). All the assays have been carried out in triplicate.
- Figure 2. SEM microphotographs of extrudates obtained by Noztek extrusion and DPE.
- Figure 3. XRD diffractograms of each of the AT-loaded DPE strands together with their pristine poweder compounds.
- Figure 4. DSC pattern of the raw materials and Noztek (A) and DPE (B) extrudates.
- Figure 5. TGA pattern of the raw material and Noztek (A) and DPE (B) extrudates.
- Figure 6. Graphical representation of the toughness *vs* the percentage w/w of AT in the performed extrudates. Extrudates prepared by DPE (A) and Noztek Pro Extrusion System (B). All the assays have been carried out in five replicates.
- Figure7. Images of binary and ternary strands with 20% and 60% of drug obtained by DPE taken by stereo microscope SMZ800N and binarized.
- Figure 8. Graphical representation of the perimeter and the inverse of the zoom ratio for 20% and 60% of drug loaded filament obtained by DPE.
- Figure 9. Graphical representation of the fractal dimension *vs* drug percentage of binary and ternary extrudates obtained by DPE (A) and Noztek Pro Extrusion System (B).